

tional strengthening reduces the probability of finding subhalos. The total effect of the presence of subhalos in external galaxies is limited to a factor 2–5.

A discussion on the minimum mass of subhalos in our Galaxy can be found in Ref. [39], where small scale clumps are considered, with masses down to $10^{-8}M_\odot$ for a DM constituted by neutralinos. An average enhancement factor of 2–5 is found, depending on the profile, while the enhancement toward the galactic center is found to be of a factor ~ 0.3 (NFW97) to ~ 0.5 (M99).

Hereafter we consider values for the cosmological factor related to an unclumpy scenario. For a clumpy halo our results can be scaled according to the previous considerations.

IV. THE SUPERSYMMETRIC FACTOR

In our study we employ a minimal supersymmetric extension of the standard model (MSSM), which is defined as an effective theory at the electroweak scale. The scheme is defined in terms of a minimal number of parameters, only the ones which are necessary to shape the essential properties of the theoretical structure of the MSSM and of its particle content. A number of assumptions are therefore imposed at the electroweak scale: (a) all squark soft-mass parameters are degenerate: $m_{\tilde{q}_i} \equiv m_{\tilde{q}}$; (b) all slepton soft-mass parameters are degenerate: $m_{\tilde{l}_i} \equiv m_{\tilde{l}}$; (c) all trilinear parameters vanish except those of the third family, which are defined in terms of a common dimensionless parameter A : $A_{\tilde{b}} = A_{\tilde{t}} \equiv Am_{\tilde{q}}$ and $A_{\tilde{\tau}} \equiv Am_{\tilde{l}}$. In addition, we employ also the standard relation at the electroweak scale between the U(1) and SU(2) gaugino mass parameters: $M_1 = (5/3)\tan^2\theta_W \simeq 0.5 M_2$, which is the low energy consequence of an underlying unification condition for the gaugino masses at the grand unified theory (GUT) scale. In this class of gaugino-universal models, the neutralino mass has a lower bound of about 50 GeV. This limit is induced by the lower bound on the chargino mass determined at LEP2 [46]: $m_{\chi^\pm} \gtrsim 100$ GeV. This is at variance with respect to effective MSSM schemes which do not possess gaugino-universality, where the neutralino mass can be as low as a few GeV's (see, for instance, Refs. [7,47] and references quoted therein). Gamma-ray detection from the annihilation of these light neutralinos has also been analyzed in Ref. [10], in the context of supergravity (SUGRA) models where gaugino nonuniversality is defined at the GUT scale.

Because of the above mentioned assumptions, the supersymmetric parameter space of our scheme consists of the following independent parameters: M_2 , μ , $\tan\beta$, m_A , $m_{\tilde{q}}$, $m_{\tilde{l}}$ and A . In the previous list of parameters μ denotes the Higgs mixing mass parameter, m_A is the mass of the CP -odd neutral Higgs boson and $\tan\beta \equiv v_t/v_b$ is the ratio of the two Higgs vacuum expectation values (VEVs) that give mass to the top and bottom quarks.

When we perform a numerical random scanning of the supersymmetric parameter space, we employ the following ranges for the parameters: $1 \leq \tan\beta \leq 50$, $100 \text{ GeV} \leq |\mu|$, $M_2 \leq 6000 \text{ GeV}$, $100 \text{ GeV} \leq m_{\tilde{q}}, m_{\tilde{l}} \leq 3000 \text{ GeV}$, $\text{sgn}(\mu) = -1, 1$, $90 \text{ GeV} \leq m_A \leq 1000 \text{ GeV}$, $-3 \leq A \leq 3$. The range on both M_2 and μ extends up to 6 TeV in order to allow us to study also very heavy neutralinos, with a mass up to about 3 TeV.

The parameter space of our effective MSSM is constrained by many experimental bounds: accelerator data on supersymmetric and Higgs boson searches [48] and on the invisible width of the Z boson, measurements of the branching ratio of the $b \rightarrow s + \gamma$ decay and of the upper bound on the branching ratio of $B_s \rightarrow \mu^+ + \mu^-$, and measurements of the muon anomalous magnetic moment $a_\mu \equiv (g_\mu - 2)/2$. The limits we use are: $2.18 \times 10^{-4} \leq BR(b \rightarrow s + \gamma) \leq 4.28 \times 10^{-4}$ [49]; $BR(B_s \rightarrow \mu^+ + \mu^-) < 7.5 \times 10^{-7}$ (95% C.L.) [50]; $-142 \leq \Delta a_\mu \times 10^{11} \leq 474$ (this 2σ C.L. interval takes into account the recent evaluations of Refs. [51,52]).

For the theoretical evaluation of $BR(b \rightarrow s + \gamma)$ and $BR(B_s \rightarrow \mu^+ + \mu^-)$ we have used the results of Ref. [53,54], respectively, with inclusion of the QCD radiative corrections to the bottom-quark Yukawa coupling discussed in Ref. [55]. We notice that gluinos do not enter directly into our loop contributions to $BR(b \rightarrow s + \gamma)$ and $BR(B_s \rightarrow \mu^+ + \mu^-)$, since we assume flavor-diagonal sfermion mass matrices. Gluinos appear only in the QCD radiative corrections to the b Yukawa coupling: in this case M_3 is taken at the standard unification value $M_3 = M_2\alpha_3(M_Z)/\alpha_2(M_Z)$, where $\alpha_3(M_Z)$ and $\alpha_2(M_Z)$ are the SU(3) and SU(2) coupling constants evaluated at the scale M_Z .

Another relevant observational constraint comes from cosmology. The recent observations on the cosmic microwave background from WMAP [56], used in combination with galaxy surveys, Lyman- α forest data, and the Sloan Digital Sky Survey Collaboration results [57], are leading to a precise knowledge of the cosmological parameters, and, in particular, of the amount of dark matter in the Universe. From the analysis of Ref. [56], we can derive a restricted range for the relic density of a cold species like the neutralinos. The density parameter of cold dark matter is bounded at 2σ level by the values: $(\Omega_{\text{CDM}}h^2)_{\text{min}} = 0.095$ and $(\Omega_{\text{CDM}}h^2)_{\text{max}} = 0.131$. This is the range for CDM that we consider in the present paper. For supersymmetric models which provide values of the neutralino relic abundance $\Omega_\chi h^2$ smaller than the minimal value $(\Omega_{\text{CDM}}h^2)_{\text{min}}$, i.e., for models where the neutralino represents a subdominant DM component, we accordingly rescale the value of the DM density: $\rho_\chi(r) = \xi \rho(r)$ with $\xi = \Omega_\chi h^2 / (\Omega_{\text{CDM}}h^2)_{\text{min}}$.

We recall that the relic abundance $\Omega_\chi h^2$ is essentially given by $\Omega_\chi h^2 \propto \langle \sigma_{\text{ann}} v \rangle_{\text{int}}^{-1}$, where $\langle \sigma_{\text{ann}} v \rangle_{\text{int}}$ is the thermal-average of the product of the neutralino annihilation

lation cross section and velocity, integrated from the freeze-out temperature in the early Universe down to the present one. The analytical calculation of σ_{ann} relies on the full set of available final states: fermion-antifermion pairs, gluon pairs, Higgs boson pairs, one Higgs boson and one gauge boson, and pairs of gauge bosons [58]. We have not included coannihilation [59] in our evaluation of the neutralino relic abundance, since in our effective supersymmetric model a matching of the neutralino mass with other particle masses is usually accidental, and not induced by some intrinsic relationship among the different parameters of the supersymmetric model like, instead, in a constrained SUGRA scheme. The inclusion of coannihilation would not change the main results of our analysis, since it would only reflect in a limited reshuffle of a small fraction of the points of the scatter plots displayed in the next sections.

A. The annihilation cross section

As already stated in Sec. II, the gamma-ray flux produced by neutralino annihilation depends on the thermal average of the neutralino self-annihilation cross section $\langle\sigma_{\text{ann}}v\rangle$ in the galactic halo at present time. The behavior of $\langle\sigma_{\text{ann}}v\rangle/m_\chi^2$, which is a relevant quantity in the calculation of the gamma-ray flux, is shown in Fig. 5 as a function of the neutralino mass and for the effective MSSM we are using. We remind that $\langle\sigma_{\text{ann}}v\rangle$ in general

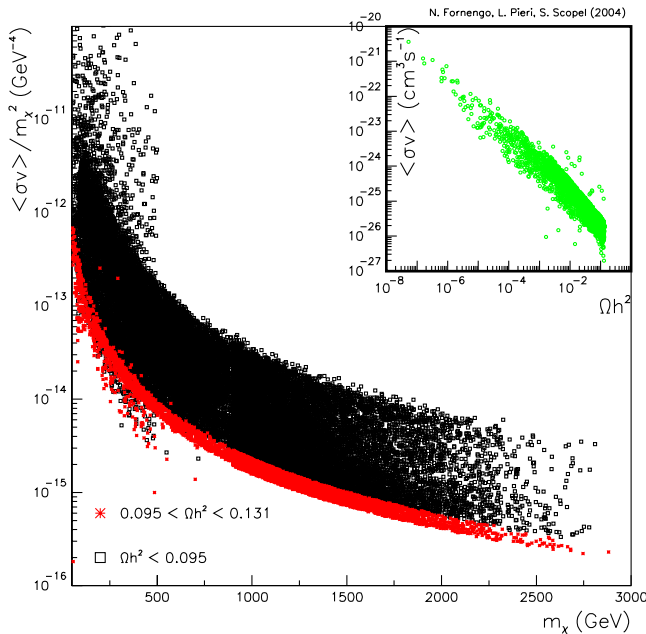


FIG. 5 (color online). The thermally-averaged annihilation cross section divided by the square of the neutralino mass m_χ as a function of m_χ in the frame of the eMSSM. Crosses show the WMAP-preferred zone for a DM dominant neutralino. In the inset the annihilation cross section at the present epoch is shown as a function of the neutralino relic abundance.

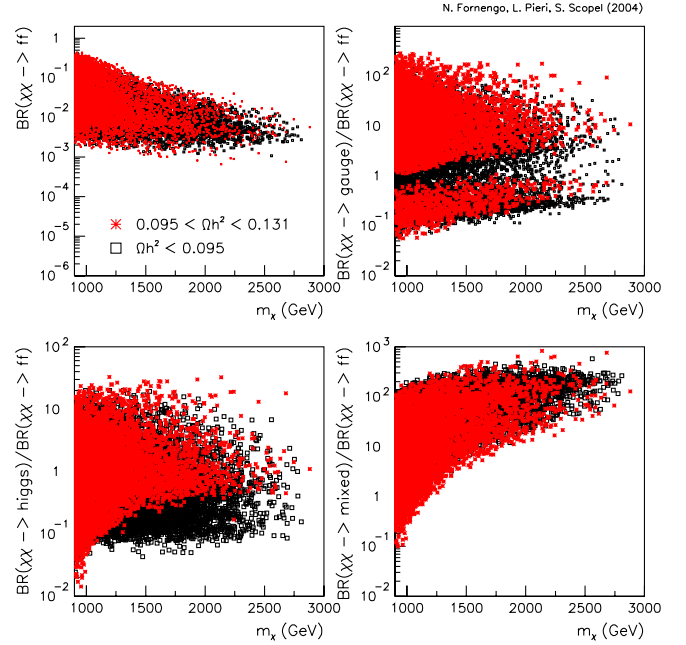


FIG. 6 (color online). The upper left panel shows the branching ratios for high mass neutralino annihilation into fermions. The other three panels show the strength of annihilation into gauge bosons (upper right), Higgs bosons (lower left), and gauge + Higgs bosons (lower right) relative to annihilation into fermions.

is different from $\langle\sigma_{\text{ann}}v\rangle_{\text{int}}$ which is responsible for the determination of the relic abundance. The two cross sections closely follow each other only for s-wave annihilation. An inverse proportionality between the gamma-ray signal and the relic abundance is therefore usually a good approximation, although deviations are present. This effect is shown in the inset of Fig. 5.

Other key ingredients for the determination of the gamma-ray signal are the branching ratios of the annihilation cross section into the different final states. For neutralinos lighter than 1 TeV the branching ratios were shown in Ref. [60]. Figure 6 extends the behavior of the branching ratios for neutralino masses higher than 1 TeV. We see that in this case the dominant channels are the two gauge bosons and the gauge boson + Higgs boson final states.

B. The photon spectrum

The diffuse photon spectrum from neutralino annihilation originates from the production of fermions, gauge bosons, Higgs bosons, and gluons. Both gauge bosons and Higgs bosons eventually decay into fermions. The hadronization of quarks and gluons, in addition to radiative processes, can produce γ rays. The main channel of production of γ rays goes through the production and subsequent decay of neutral pions. The contribution to the γ -ray spectrum from production and decay of mesons other than pions (mostly η , η' , charmed, and bottom

mesons) and of baryons is usually subdominant as compared to π^0 decay and it has been neglected. Neutralino annihilation into lepton pairs can also produce γ rays from electromagnetic showering of the final state leptons. This process can be dominant for $E_\gamma \lesssim 100$ MeV, when the neutralino annihilation process has a sizable branching ratio into lepton pairs. In the case of production of τ leptons, their semihadronic decays also produce neutral pions, which then further contribute to the gamma-ray flux.

As discussed in Ref. [7], we have evaluated the gamma-ray fluxes originating from hadronization and radiative processes by means of a Monte Carlo simulation with the PYTHIA package [61]. In the present paper we extend that analysis by giving explicit fits to our numerical distributions which are valid for the energies of interest in the current analysis, i.e., for photon energies $E > 10$ GeV. When a flux is presented for energies below 10 GeV, the numerical analysis has been used.

The differential spectra of photons from DM annihilation have been parametrized as follows:

$$\frac{dN_\gamma^i}{dx} = \eta x^a e^{b+cx+dx^2+ex^3} \quad (10)$$

where $x = E_\gamma/m_\chi$ and i identify quarks, W , Z and gluons. The value of η is two for W , Z and top quark final states, and one otherwise. In the case of τ leptons, the functional

TABLE V. Fitted parameters of Eq. (10) for the annihilation of neutralinos into quarks and gauge bosons, calculated for $m_\chi = 500$ GeV and $m_\chi = 1$ TeV. Fits obtained with these parameters are valid down to $E = 10$ GeV.

	$m_\chi = 500$ GeV			$m_\chi = 1$ TeV		
	u	s	t	u	s	t
a	-1.5	-1.5	-1.5	-1.5	-1.5	-1.5
b	0.047	0.093	-0.44	0.0063	0.040	-0.45
c	-8.70	-9.13	-19.50	-8.62	-8.84	-19.05
d	9.14	4.49	22.96	8.53	2.77	21.96
e	-10.30	-9.83	-16.20	-9.73	-7.71	-15.18
	d	c	b	d	c	b
a	-1.5	-1.5	-1.5	-1.5	-1.5	-1.5
b	0.047	0.25	0.48	0.0063	0.17	0.37
c	-8.70	-10.76	-16.87	-8.62	-10.23	-16.05
d	9.14	4.25	21.09	8.53	2.13	18.01
e	-10.30	-8.70	-22.49	-9.73	-7.00	-19.50
	W	Z	g	W	Z	g
a	-1.5	-1.5	-1.5	-1.5	-1.5	-1.5
b	-0.85	-0.76	0.55	-0.95	-0.83	0.48
c	-11.07	-11.96	-20.78	-9.86	-11.175	-20.51
d	9.47	8.65	26.79	6.25	6.5902	24.42
e	-6.80	-5.21	-22.80	-4.37	-3.6468	-19.56

TABLE VI. Parameters of Eq. (11) for the annihilation of neutralinos into τ leptons, calculated for $m_\chi = 500$ GeV and $m_\chi = 1$ TeV. Fits obtained with these parameters are valid down to $E = 10$ GeV.

	$m_\chi = 500$ GeV	$m_\chi = 1$ TeV
a_τ	-1.34	-1.31
b_τ	6.27	6.94
c_τ	0.89	-4.93
d_τ	-4.90	-0.51
e_τ	-5.10	-4.53

form for the differential number of photons is:

$$\frac{dN_\gamma^\tau}{dx} = x^{a_\tau} (b_\tau x + c_\tau x^2 + d_\tau x^3) e^{e_\tau x}. \quad (11)$$

The values of the parameters of the fits are given in Tables V and VI for the two representative values of $m_\chi = 500$ GeV and $m_\chi = 1$ TeV.

In Fig. 7 we show an example of photon spectra originated by neutralino annihilation into different pure final states of a neutralino with $m_\chi = 1$ TeV. We see that at lower energies the dominant contribution is given by the γ rays coming from the hadronization of quarks and gluons. The spectra coming from gauge bosons are somewhat harder, while the hardest ones are given by the τ lepton. In the case of Higgs bosons, the spectra are mainly

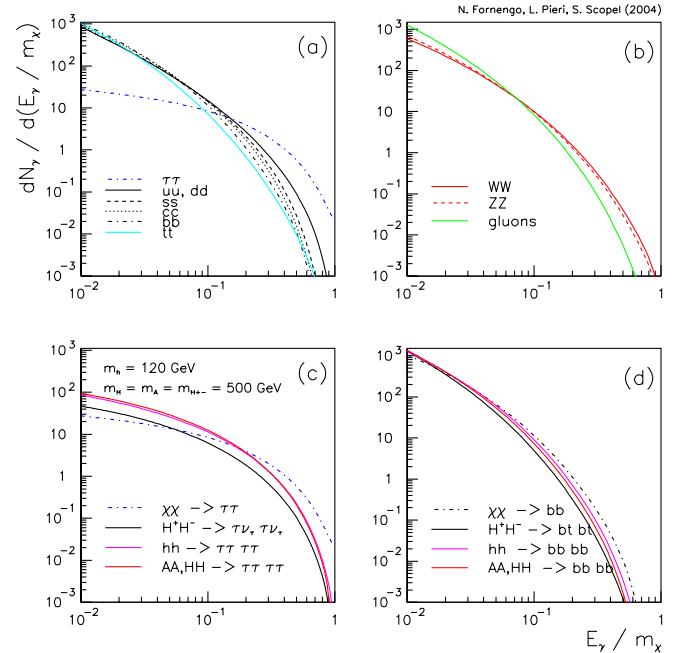


FIG. 7 (color online). The photon spectrum from an $m_\chi = 1$ TeV neutralino annihilation into: (a) leptons, (b) gauge bosons, (c) Higgs bosons decaying into τ 's, and (d) Higgs bosons decaying into b 's. For each curve a branching ratio of 100% in that channel has been considered.